



HAL
open science

Terahertz plasmons in doped HgTe quantum well heterostructures: dispersion, losses, and amplification

V. Ya. Aleshkin, A. Dubinov, V. Gavrilenko, F Teppe

► **To cite this version:**

V. Ya. Aleshkin, A. Dubinov, V. Gavrilenko, F Teppe. Terahertz plasmons in doped HgTe quantum well heterostructures: dispersion, losses, and amplification. *Applied optics*, 2021, 60 (28), pp.8991-8998. 10.1364/AO.438501 . hal-03824987

HAL Id: hal-03824987

<https://hal.science/hal-03824987>

Submitted on 26 Oct 2022

HAL is a multi-disciplinary open access archive for the deposit and dissemination of scientific research documents, whether they are published or not. The documents may come from teaching and research institutions in France or abroad, or from public or private research centers.

L'archive ouverte pluridisciplinaire **HAL**, est destinée au dépôt et à la diffusion de documents scientifiques de niveau recherche, publiés ou non, émanant des établissements d'enseignement et de recherche français ou étrangers, des laboratoires publics ou privés.

Terahertz plasmons in doped HgTe quantum well heterostructures: dispersion, losses and amplification

V.YA. ALESHKIN,^{1,2} A.A. DUBINOV,^{1,2,*} V.I. GAVRILENKO^{1,2} AND F. TEPPE³

¹*Institute for Physics of Microstructures RAS, GSP-105, Nizhny Novgorod, 603950, Russia*

²*Lobachevsky State University of Nizhny Novgorod, 23 Gagarina av., Nizhny Novgorod, 603950, Russia*

³*Laboratoire Charles Coulomb, Université de Montpellier, Centre National de la Recherche Scientifique, Montpellier, 34095, France*

*sanya@ipmras.ru

Abstract: We have calculated two-dimensional plasmon energy spectra in HgTe/CdHgTe quantum wells with normal, gapless and inverted energy spectra with different electron concentrations and taking into account spatial dispersion of electron polarizability and plasmon interaction with the optical phonons. The spectra of the absorption coefficients of two-dimensional plasmons are found. It is shown that an increase of electron concentration in a quantum well leads to a decrease in the plasmon absorption coefficient. We have calculated the probabilities to recombine via the plasmon emission for nonequilibrium holes. The threshold concentrations of the nonequilibrium holes, above which the plasmon amplification is possible, have been calculated for various electron concentrations. It is shown that the presence of equilibrium electrons can significantly reduce the threshold hole concentration required for amplification of plasmon in the terahertz wavelength region. The dependencies of threshold hole concentration on electron concentration for different quantum wells are discussed. Gain spectra of the two-dimensional plasmon are calculated.

© 2021 Optical Society of America

1. Introduction

In the last decade, the possibility of amplifying two-dimensional plasmons in graphene has been intensively studied [1-6]. The attractiveness of this idea is due to the possibility of generating and amplifying plasmons in the terahertz frequency range, in the absence of any special waveguides, and at high mode gain factors ($\sim 10^5 \text{ cm}^{-1}$). The latter opens up possibilities for creating compact radiation sources with a size of the order of several microns. Despite the fact that the first experimental evidence has already been obtained on the possibility of amplifying plasmons in graphene [4], there are serious difficulties in the way of realizing this possibility. First of all, these are very short lifetimes of nonequilibrium carriers in graphene, which lie in the picosecond time range [7], and therefore high excitation powers are required to create the inverse population of the bands, which is necessary for amplifying plasma oscillations. In addition, to date, the technology of creating graphene with high electron mobility, which is required for the plasmon generation, is poorly developed.

On the contrary, the technology of molecular beam epitaxy of quantum wells (QWs) in HgTe/CdHgTe material system is currently well developed and makes it possible to obtain QWs with a band gap from zero to several hundreds of meV [8]. This system has more flexibility for creating of the desired electronic spectrum compared to graphene structures. In addition, the lifetimes of nonequilibrium charge carriers in HgTe quantum wells are orders of magnitude longer than in graphene (see, for example, [9,10]), which is another advantage of this system. The authors of Ref. 11 drew attention to these advantages and proposed to use these structures to amplify 2D plasmons. However, the authors of Ref. 11 considered the case of undoped quantum wells only (i.e., the concentration of nonequilibrium electrons was equal to that of nonequilibrium holes), neglected the frequency dispersion of polarizability, and did

not consider the interaction of plasmons with longitudinal optical (LO) phonons. In this work, we study the influence of the listed factors on the properties of two-dimensional plasmons: the equilibrium electron concentration in the QW, the frequency dispersion of the electronic polarizability, and the interaction with optical phonons.

In our previous work [12], an important role in the recombination of nonequilibrium charge carriers in undoped HgTe QW processes with the emission of plasmons was shown. However, for doped structures, this issue has not been practically studied to date.

The article is organized as follows. In the first part of the work, the model that was used to describe plasmons is presented, the results of calculations of the spectra of the coupled plasmon-LO phonon modes and the absorption coefficients for QWs with normal and inverted band structures, as well as for a gapless QW for various equilibrium electron concentrations in the QW, are presented.

In the next section, the processes of recombination of nonequilibrium holes with the emission of plasmons are considered. In the third part of the work, the question of the influence of the concentration of equilibrium electrons on the value of the threshold concentration of holes, above which amplification and generation of plasmons is possible, is studied. The main results of this work are summarized in Conclusions.

2. Dispersion laws of plasmons

The dependence of the frequency of a two-dimensional plasmon ω on its wave vector q can be found from the relation [13]:

$$1 + \frac{2\pi}{\kappa(\omega)} \chi(q, \omega) \sqrt{q^2 - \left(\frac{\omega}{c}\right)^2} \kappa(\omega) = 0 \quad (1),$$

where $\kappa(\omega)$ is the dielectric constant of the barrier layers, $\chi(q, \omega)$ is the polarizability of the electron gas in the QW, and c is the light velocity in the free space. Generalizing the Lindhard formula [14], we can obtain the following expression for the polarizability of a two-dimensional electron-holes system (see the appendix in Ref. 15):

$$\chi(q, \omega) = \frac{e^2}{q^2 (2\pi)^2} \times \sum_{s, s'} \int \frac{(f_s(\mathbf{k}) - f_{s'}(\mathbf{k} + \mathbf{q})) |\psi_{\mathbf{k}+\mathbf{q}, s'}^+ \psi_{\mathbf{k}, s}|^2}{\varepsilon_{s'}(\mathbf{k} + \mathbf{q}) - \varepsilon_s(\mathbf{k}) - \hbar\omega - i\hbar\nu_{s', \mathbf{k}+\mathbf{q}; s, \mathbf{k}}} d^2k \quad (2),$$

where \hbar is Planck's constant, indices s and s' denote the number of the subband, including the spin index, $\varepsilon_s(\mathbf{k})$ is the energy of an electron with a wavevector \mathbf{k} in the s -th subband, $f_s(\mathbf{k})$ is the electron distribution function, $-e$ is the electron charge, $\nu_{s', \mathbf{k}+\mathbf{q}; s, \mathbf{k}}$ are the phase relaxation frequency for the density matrix component $\rho_{s', \mathbf{k}+\mathbf{q}; s, \mathbf{k}}$. If the wave function of an electron in the s -th subband is represented as: $\psi_{\mathbf{k}, s}(\mathbf{r}) = \psi_{\mathbf{k}, s}(z) \exp(i\mathbf{k}\mathbf{r}) / \sqrt{S}$, where z is the coordinate of the normal to the QW, S is the area of the QW, then the last factor in the integrand (2) takes the form: $|\psi_{\mathbf{k}+\mathbf{q}, s'}^+ \psi_{\mathbf{k}, s}| = \left| \int dz \psi_{\mathbf{k}+\mathbf{q}, s'}^+(z) \psi_{\mathbf{k}, s}(z) \right|$.

In calculating the polarizability, the electron distribution function in the s -th subband was assumed to be as follows:

$$f_s(\mathbf{k}) = \left(1 + \exp\left(\frac{\varepsilon_s(\mathbf{k}) - F_{js}}{k_B T}\right) \right)^{-1} \quad (3),$$

where F_{js} is the chemical potential in the s -th subband ($js = c$ if s belongs to the conduction subbands and $js = v$ if s belongs to the valence subbands), k_B is the Boltzmann constant, T is the

temperature. The values $F_{c,v}$ were found from the given concentrations of electrons and holes, correspondingly. In the case when there are nonequilibrium holes in the system, the chemical potential for all subbands of the valence band was assumed to be the same and equal to F_v , two upper holes subbands being taken into when summed in the expression (2). The corresponding distribution (3) in these hole subbands was characterized by the effective temperature T_h , which could be different from the electron temperature.

In what follows, we will assume that the barriers are formed by the $\text{Cd}_{0.7}\text{Hg}_{0.3}\text{Te}$ solid solution, that is typical for the experimentally studied samples (see e.g. Ref. 8-10). In addition, for this composition of the solid solution, there is an approximation of the dielectric constant obtained from the fitting to the measured reflection spectrum [16]:

$$\kappa(\omega) = \kappa_\infty + \sum_{j=1}^8 \frac{S_j \omega_{jT}^2}{\omega_{jT}^2 - \omega^2 - i\Gamma_j \omega} \quad (4),$$

In our calculations we used values of κ_∞ , S_j , ω_{jT}^2 , Γ_j from Ref. 16.

The spectra of electrons in the quantum well were calculated using the 4-band Kane model (Hamiltonian 8x8) with allowance for deformation effects. For simplicity, we did not take into account the effects due to the absence of an inversion center in the crystal lattice and a decrease in symmetry at heterointerfaces, which remove the spin degeneracy. Therefore, in our model, the energy subbands are twofold degenerate in spin. Note that experimental measurements of the spectrum of electronic levels in the conduction band in almost gapless QWs did not reveal spin splitting [17], despite theoretical predictions [18]. Details of the calculations of the electronic spectrum can be found in Ref. 19. We consider the $\text{HgTe}/\text{Cd}_{0.7}\text{Hg}_{0.3}\text{Te}$ structures grown on the (013) plane, since just in these structures the stimulated emission in the mid and far IR/THz ranges has been studied experimentally [20-22].

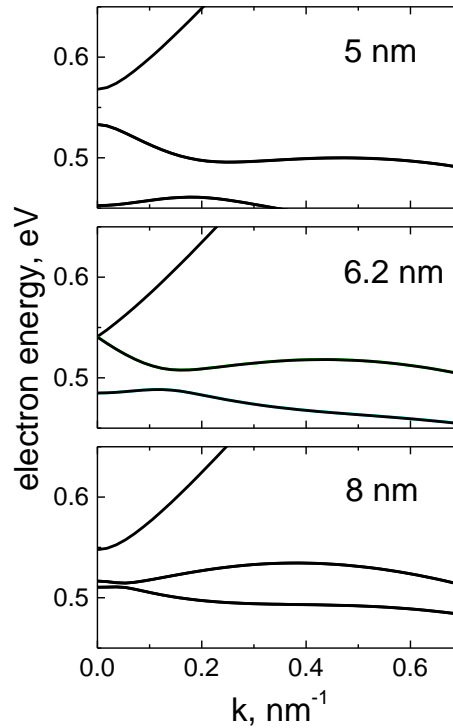


Fig. 1. Energy spectra in 3 $\text{HgTe}/\text{Cd}_{0.7}\text{Hg}_{0.3}\text{Te}$ QWs of 5, 6.2 and 8 nm width. $\mathbf{k}||[100]$.

We will consider plasmons in narrow-gap quantum wells 5 nm, 6.2 nm, and 8 nm wide. The temperature of the lattice and electrons in the conduction band was everywhere assumed to be 4.2 K. The band gap in the 5 nm QW is 35 meV, QW 6.2 nm wide is gapless, and an 8 nm QW has an indirect-gap "inverted" band structure (the band gap at $k = 0$ is 31 meV) [19]. Fig. 1 shows the calculated electronic spectra in these three wells.

When calculating the polarizability by formula (2), we took into account the two ground subbands differing in spin in the conduction band, and the two ground subbands differing in spin in the valence band. We did not take into account the transitions between the ground and excited electron subbands in the conduction band, since the distances between the ground and excited subbands are large (236 meV at $k = 0$ for 8 nm QW, 321 for 6.2 nm QW, and 374 for 5 nm QW). For this reason, transitions of electrons between the ground and excited electronic subbands in the conduction band with the participation of the considered plasmons are impossible. Hole transitions between the ground and excited subbands in the valence band were also disregarded, since they are insignificant for the problems considered below.

It is well known (see Problem 6.10 in Ref. 23) that as a result of the interaction of a bulk plasmon and a longitudinal optical phonon, two coupled plasmon-LO phonon modes appear. The frequency of the low-frequency mode is lower than that of the transverse optical (TO) phonon [23], and the frequency of the high-frequency mode is higher than the frequency of the LO phonon. A similar picture takes place for two-dimensional plasmons. Fig. 2 shows the dependences of the energy of the high-frequency plasmon-LO phonon mode on the wave vector for the three considered QWs and three electron concentrations. The figure shows that the dispersion dependences of the modes are very close for all considered wells. With an increase in the QW width from 5 nm to 6.2 nm, the mode frequency slightly increases, and with further growth from 6.2 nm to 8 nm, it slightly decreases. Similar patterns are valid for the low-frequency mode (see Fig. 3). Note that, due to the weak anisotropy of the electron energy in the conduction band, the spectrum of the plasmon-LO phonon modes is also practically isotropic, i.e. does not depend on the direction of the wave vector.

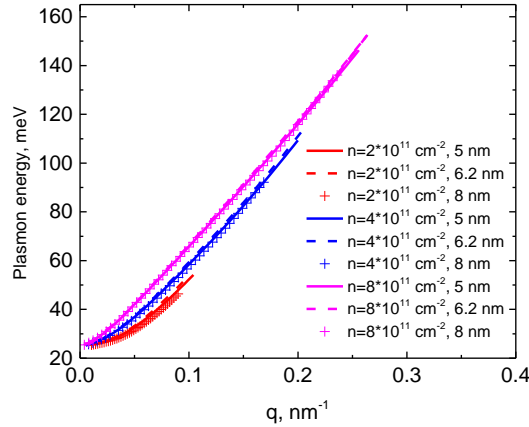


Fig. 2. Dependence of the energy of the high-frequency plasmon-LO mode on the wave vector for three electron concentrations in 5, 6.2 and 8 nm wide QWs. $T = 4.2$ K, $\hbar\nu_{s^*k+q,s,k} = 1$ meV.

For calculations, we used two values of $\hbar\nu_{s^*k+q,s,k} = 1$ meV and $\hbar\nu_{s^*k+q,s,k} = 0.1$ meV. If we assume that $\nu_{s^*k+q,s,k}$ corresponds to the scattering frequency of the electron momentum, then the corresponding electron mobilities should be in the range $3.6 \cdot 10^4 - 3.6 \cdot 10^5$ cm²/V·s, which is in reasonable agreement with the experimentally measured values of the mobility in similar

structures (see, for example, Ref. 24). Note that the dependences of the real part of the frequency on the wave vector for both high-frequency and low-frequency plasmon-LO phonon modes are practically the same for the two values $\hbar v_{s,\mathbf{k}+\mathbf{q};s,\mathbf{k}}$ used.

Intraband absorption of plasmons (Landau damping) leads to their strong decay and, where this absorption is possible, plasmons are poorly defined. Landau damping begins when the most energetic electrons can absorb a plasmon with a wave vector parallel to the electron momentum. At low temperatures, these are electrons at the Fermi level. The wavevector of the plasmon-LO phonon mode for the intraband absorption of the plasmon must satisfy the condition [11]:

$$\varepsilon(k_F + q) = \varepsilon(k_F) + \hbar\omega(q) \quad (5),$$

where k_F is the wave vector of the electron at the Fermi level.

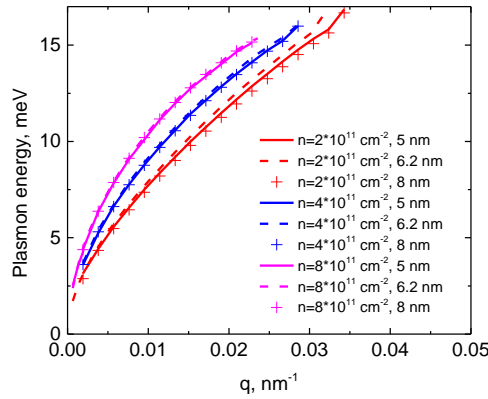


Fig. 3. Dependence of the energy of the low-frequency plasmon-LO mode on the wave vector for three electron concentrations in 5, 6.2 and 8 nm wide QWs. $T = 4.2$ K, $\hbar v_{s,\mathbf{k}+\mathbf{q};s,\mathbf{k}} = 1$ meV.

The right edges of the end of the dependence of the mode energy on the wave vector in Figs. 2,3 correspond to the beginning of Landau damping. It can be seen from the figures that for the high-frequency mode the wavevector corresponding to the onset of Landau damping increases with the electron concentration. This is due to an increase in the phase velocity of the mode with the electron concentration. For the low-frequency mode, another regularity is observed: with increasing concentration, the wave vector corresponding to the onset of Landau damping decreases.

Let us now consider the spectra of the absorption coefficients. As is known, the absorption coefficient is equal to the doubled imaginary part of the wavevector. In general, frequency is a complex analytical function of a complex wavevector. When solving (1), we find the complex frequency as a function of the real wave vector q . Let us show how to find the imaginary part of the wavevector for the real frequency from this dependence. In a small neighborhood of the real wavevector q_0 , the following expansion is valid:

$$\omega(q) \approx \omega(q_0) + v_g(q_0)(q - q_0), \quad v_g(q) = \frac{d\omega}{dq} \quad (6),$$

where $v_g(q)$ is the complex group velocity. In the neighborhood of q_0 on the complex plane, we find a point q at which the following condition is satisfied: the frequency is equal to the real part $\omega(q_0)$, i.e. $\omega(q) = \text{Re}(\omega(q_0))$. Note that the imaginary part of the frequency at a point q_0 is small compared to the real part of the frequency (the difference is more than an order of magnitude).

From the above condition imposed on q and from (6) it follows that $v_g(q_0)(q - q_0) = -i \text{Im}(\omega(q_0))$. From this equality we find $\text{Im}(q) = -\text{Im}(\omega(q_0)) \text{Re}(v_g^{-1}(q_0))$. Since the absorption coefficient is equal to the doubled imaginary part of the wave vector, the absorption coefficient as a function of the real frequency can be written as:

$$\alpha(\text{Re}(\omega(q_0))) = -2 \text{Im}(\omega(q_0)) \text{Re}(v_g^{-1}(q_0)) \quad (7).$$

Fig. 4 shows the spectra of the absorption coefficients of the plasmon-LO phonon modes. Solid lines correspond to $\hbar v_{s^*k+q,s,k} = 1$ meV, and dashed lines to $\hbar v_{s^*k+q,s,k} = 0.1$ meV. Red lines correspond to $n = 2 \cdot 10^{11}$ cm⁻², blue - to $n = 4 \cdot 10^{11}$ cm⁻², magenta - to $n = 8 \cdot 10^{11}$ cm⁻².

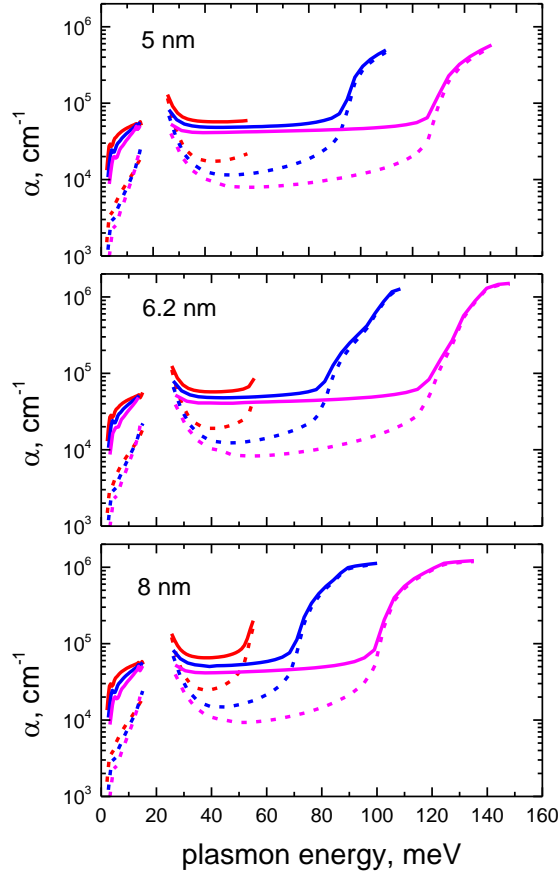


Fig. 4. Spectra of absorption coefficients of plasmon-LO modes in three QWs. Solid lines correspond to $\hbar v_{s^*k+q,s,k} = 1$ meV, and dashed lines to $\hbar v_{s^*k+q,s,k} = 0.1$ meV. Red lines correspond to $n = 2 \cdot 10^{11}$ cm⁻², blue - $n = 4 \cdot 10^{11}$ cm⁻², magenta - $n = 8 \cdot 10^{11}$ cm⁻². $T = 4.2$ K.

The absorption of low-frequency mode, with the exception of the region close to the *Reststrahlen* band, is completely determined by absorption on free carriers even in a gapless QW 6.2 nm wide and therefore drops with decreasing $\hbar v_{s^*k+q,s,k}$. Absorption due to interband transitions is impossible here because of the Burstein-Moss effect. In the vicinity of the *Reststrahlen* band for both the high-frequency and the low-frequency modes, phonon absorption plays a significant role in absorption; therefore, here the change in $\hbar v_{s^*k+q,s,k}$ is not as significant as far from the the *Reststrahlen* band. Comparing Fig. 2,3 and Fig. 4 one can see that the free carrier absorption increases with a decrease in the group velocity of the plasmon-

LO phonon modes. For the low-frequency mode, the group velocity decreases with increasing mode energy, and for the high-frequency mode, with decreasing mode energy.

For high-frequency mode, the increase in the absorption coefficient at high energies is due to the contribution from the transitions of electrons from the valence band to the conduction band (except for the 5 nm QW at $n = 2 \cdot 10^{11} \text{ cm}^{-2}$). The threshold energy corresponding to the switching on the interband absorption, increases with the electron concentration, what is due to the Burstein-Moss effect. As easy to see from Fig. 4, the increase in the absorption coefficient due to the contribution of the interband transitions can be by an order of magnitude. Note that for both types of modes, absorption decreases with an increase in the electron concentration.

3. Electron-hole recombination with plasmon emission

In narrow-gap QWs, the rate of recombination with the emission of plasmons can exceed those of radiative and Auger recombinations [12]. Hereinafter, for brevity, we will use the term plasmon recombination to denote recombination with the excitation of the plasmon-LO phonon modes. Plasmon recombination processes for undoped HgTe QWs were considered in Ref. 12. In this section, we will consider the plasmon recombination of nonequilibrium holes (generated, say, by interband optical excitation) in doped HgTe QWs with a high concentration of equilibrium electrons. To find the probability of such a recombination, it is necessary to quantize the plasmon-LO phonon modes. For this, we will use the results of Ref. 12 in which this quantization was carried out. The expression for the operator of the vector potential of the electromagnetic field of the plasmon-LO phonon mode has the form [12]:

$$\mathbf{A}_q = -\frac{c\mathbf{q}}{\omega} \sqrt{\frac{2\hbar}{Sq^2}} \left(\frac{\partial \chi}{\partial \omega} \right)^{-1} \times \left(c_q \exp(i\mathbf{q}\mathbf{r} - i\omega t) + c_q^+ \exp(-i\mathbf{q}\mathbf{r} + i\omega t) \right) \quad (8),$$

where c_q, c_q^+ are the plasmon creation and annihilation operators. Using (8) and the Fermi golden rule, we can obtain the following expression for the probability of transition of an electron with the wavevector $\mathbf{k}+\mathbf{q}$ from the i -th subband of the conduction band to the empty state with the wavevector \mathbf{k} of the j -th subband of the valence band with the emission of a plasmon with the wavevector \mathbf{q} :

$$W_{i,j}(\mathbf{k}) = \frac{e^2}{2\pi} \int d^2q \left\{ \frac{|\mathbf{v}_{i,j}\mathbf{q}|^2}{q^2\omega^2} \left(\frac{\partial \chi(q,\omega)}{\partial \omega} \right)^{-1} \times \delta(\varepsilon_i(\mathbf{k}+\mathbf{q}) - \varepsilon_j(\mathbf{k}) - \hbar\omega) f_i(\mathbf{k}+\mathbf{q}) \right\} \quad (9),$$

where $\mathbf{v}_{i,j}$ is the matrix element of the velocity operator between the initial and the final electron states. The meaning of $W_{i,j}(\mathbf{k})$ is the probability of recombination of a hole with the wave vector $-\mathbf{k}$ with the emission of a plasmon.

The total rate of the considered recombination can be represented as:

$$R = \frac{1}{(2\pi)^2} \sum_{i,j} \int d^2k W_{i,j}(\mathbf{k}) (f_i(\mathbf{k}+\mathbf{q}) - f_j(\mathbf{k})) = pW(p) \quad (10),$$

where p is the concentration of nonequilibrium holes, $W(p)$ is the ensemble average probability of plasmon recombination, and the summation is carried out over all the initial and final states of the electron. Since in this work we will consider low concentrations of nonequilibrium carriers (less than $3 \cdot 10^{10} \text{ cm}^{-2}$), they practically do not affect the dependence $\omega(q)$. In addition, due to the low concentration of holes and their low effective temperature (in what follows we will assume that it does not exceed 77 K), they occupy a small vicinity of the point $\mathbf{k} = 0$, where the hole spectrum is almost isotropic. Therefore, we can introduce the probability of

recombination of holes with wave vector k , averaged over the initial and final spin states and over the direction of \mathbf{k} :

$$w(k) = \frac{1}{4\pi} \sum_{i,j} \int d\varphi_k W_{i,j}(\mathbf{k}) \quad (11),$$

where φ_k is the angle between the \mathbf{k} direction and the x axis [100].

In a QW with an inverted band structure and indirect band gap under consideration, holes occupy side valleys. For them, plasmon recombination is forbidden by the energy and momentum conservation laws; therefore, in this section, we do not consider such wells.

Let's start with the recombination in a 5 nm wide QW. Since in this well the band gap is greater than the energy of the low-frequency plasmon-LO phonon mode, only the high-frequency mode can participate in the plasmon recombination. Fig. 5 shows the dependences $W(p)$ for different electron concentrations at two effective temperatures of nonequilibrium holes $T_h = 4.2$ K and $T_h = 77$ K.

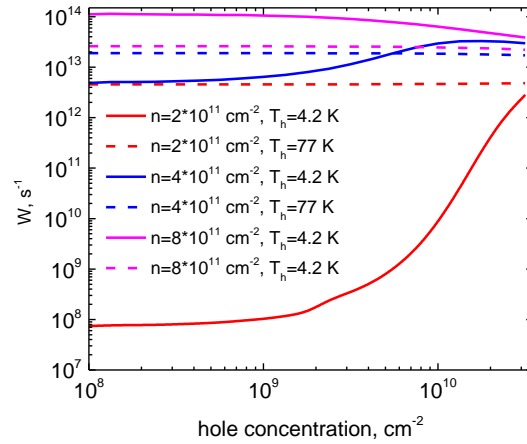


Fig. 5. Hole concentration dependence of ensemble average probability of the plasmon recombination $W(p)$ in a 5 nm wide QW.

It can be seen from the Fig.5 that at an effective hole temperature $T_h = 4.2$ K (solid lines), $W(p)$ increases with the hole concentration for electron concentrations of $2 \cdot 10^{11} \text{ cm}^{-2}$ and $4 \cdot 10^{11} \text{ cm}^{-2}$ and decreases for the electron concentration of $8 \cdot 10^{11} \text{ cm}^{-2}$. At $T_h = 77$ K, the recombination probability W weakly depends on the hole concentration. Note that as T_h changes from 4.2 K to 77 K, the probability $W(p)$ for low hole concentrations increases by four orders of magnitude.

In order to explain such regularities, let us consider the dependences of the recombination probability on the hole wave vector $w(k)$ shown in Fig. 6. As easy to see from Fig. 6, for electron concentrations of $2 \cdot 10^{11} \text{ cm}^{-2}$ and $4 \cdot 10^{11} \text{ cm}^{-2}$, at $T_h = 4.2$ K holes with small wave vectors (low kinetic energies) cannot participate in the plasmon recombination. With increasing the hole concentration p (and therefore hole Fermi energy), the fraction of holes involved in recombination increases giving rise to a sharp increase in the recombination probability. On the contrast, at $T_h = 77$ K, the hole gas is practically non-degenerate. In this case, the difference between the distribution functions of electrons in the conduction and valence bands can be set equal to:

$$f_i(\mathbf{k} + \mathbf{q}) - f_j(\mathbf{k}) \approx 1 - f_j(\mathbf{k}) \approx \exp\left(\frac{\varepsilon_j(\mathbf{k}) - F_v}{k_B T_h}\right) \quad (12),$$

and it can be seen from (10) that for a nondegenerate hole gas $W(p)$ should not depend on p since the only p -dependent factor $\exp(-F_v/k_B T_h) \sim p$ can be taken off the integral (10).

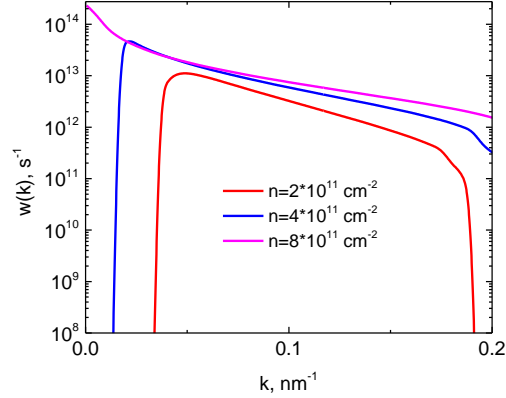


Fig. 6. Dependence of the hole recombination probability $w(k)$ in a 5 nm wide QW at $T_h=4.2$ K.

A completely different situation at $T_h = 4.2$ K takes place for $n = 8 \cdot 10^{11} \text{ cm}^{-2}$. In this case, the maximum $w(k)$ is at $k = 0$ (see Fig. 6), and therefore, at $T_h = 4.2$ K, the probability $W(p)$ decreases with increasing hole concentration p (Fig. 5). This is also the reason that $W(p)$ at $T_h = 77$ K is less than at $T_h = 4.2$ K for this electron concentration since the hole distribution function at $k \approx 0$ drops with the effective temperature increase.

As easy to see from Fig. 6, with a decrease in the electron concentration, the interval of wave vectors in which holes can recombine narrows. When the electron concentration is less than $1.1 \cdot 10^{11} \text{ cm}^{-2}$, this interval vanishes and plasmon recombination becomes impossible. The reason for this is the impossibility of fulfilling the energy-momentum conservation law because the plasmon energy is less than the effective band gap $\varepsilon_{\text{eff}}(q)$ (see Ref. 12).

Let us now consider plasmon recombination in a 6.2 nm wide QW. In this case, both high- and low-frequency plasmon-LO phonon modes can participate in the recombination. Fig. 7 shows the dependences of average probability of plasmon recombination W on the hole concentration p for a 6.2 nm wide QW. It can be seen that at $T_h = 4.2$ K, W increases with an increase in the hole concentration and decreases with an increase in the electron concentration. To explain these regularities, let us consider the $w(k)$ dependences for the high-frequency (main figure) and low-frequency (inset) modes shown in Fig. 8. As easy to see, only the low-frequency plasmon-LO phonon mode can participate in the recombination of holes with small wave vectors. On the contrary, only the high-frequency mode can participate in the recombination of holes with $k > 0.05 \text{ nm}^{-1}$.

Note that the value of the minimum wave vector of the hole, at which the recombination with the participation of the high-frequency mode is activated, increases with an increase in the electron concentration. This pattern can be understood by graphically analyzing the energy-momentum conservation laws, taking into account the dependence of the high-frequency mode on the wave vector and the linear dispersion law of electrons and holes in a gapless QW. As in the 5 nm wide QW at $T_h = 77$ K, the probability W weakly depends on the concentration of nonequilibrium holes p .

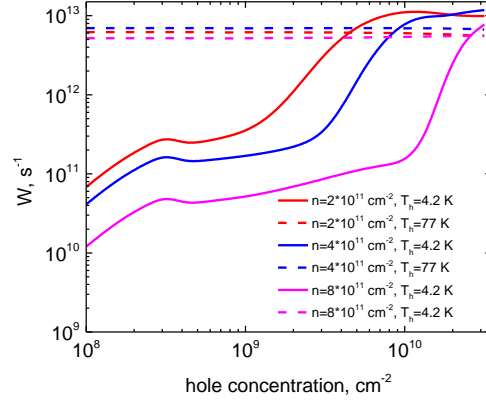


Fig. 7. Hole concentration dependence of ensemble average probability of plasmon recombination $W(p)$ in a 6.2 nm wide QW.

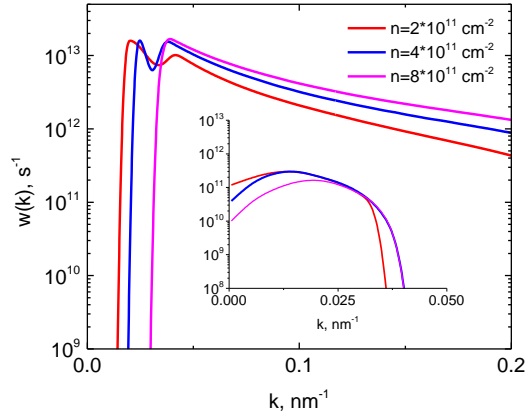


Fig. 8. Dependence of the hole recombination probability $w(k)$ in a 6.2 nm wide QW at $T_h = 4.2$ K for high-frequency plasmon-LO mode. In the insert: $w(k)$ dependence for low-frequency plasmon-LO mode.

4. Amplification of plasmons in doped quantum wells under condition of population inversion

Let us now consider the possibility of amplifying the plasmon-LO phonon modes in the structures under consideration. Amplification of plasmons is possible under conditions when the concentration of nonequilibrium carriers is high enough to create an inverted band population. In this case, the amplification of plasmons occurs due to the transitions of electrons from the conduction band to the valence band with the emission of a plasmon. In undoped structures this issue was studied in Ref. 11,15. As mentioned in the Introduction, there are two advantages of coherent generation of plasmons over the generation of waveguide modes. The first advantage is that there is no need to create a special waveguide, which is usually created

in the terahertz quantum-cascade lasers with the help of metal coatings, which lead to additional losses (see, e.g., Ref. 25). The second advantage consists in large ($\sim 10^4$ - 10^5 cm⁻¹) mode gain [11,15], which opens the way to the creation of micron-sized terahertz lasers.

An important characteristic of a structure intended for the coherent generation of plasmons is the threshold concentration of nonequilibrium carriers. Upon reaching this concentration, the amplification of plasmons is equal to the losses. When the concentration of nonequilibrium carriers exceeds the threshold concentration, amplification and coherent generation of plasmons is possible. Since lasing is possible only in direct-gap structures, in this section we will consider only 6.2 and 5 nm wide quantum wells.

To find the threshold concentration, it is necessary to calculate the spectrum of the absorption coefficient at various concentrations of nonequilibrium carriers. The threshold concentration corresponds to the appearance of zero absorption in the spectrum. Fig. 9 shows the threshold hole concentrations for 5 nm and 6.2 nm wide QWs for three electron concentrations. It can be seen from the figure that amplification of both high-frequency and low-frequency modes is possible in a gapless 6.2 nm QW. For the two values $\hbar v_{s^*k+q;s,k}$ considered, the generation of the low-frequency mode is possible only for $\hbar v_{s^*k+q;s,k} = 0.1$ meV; the threshold hole concentrations being lower than those for the high-frequency mode.

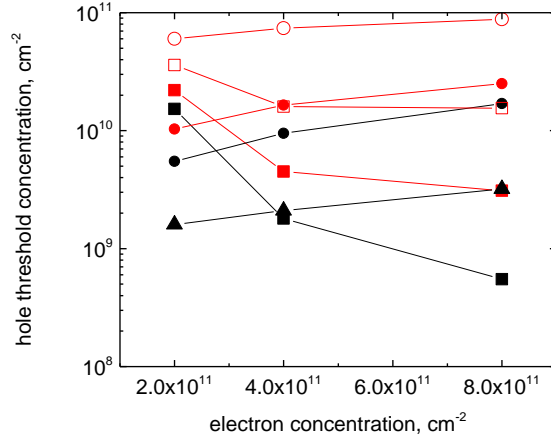


Fig. 9. Threshold concentrations of nonequilibrium holes for three values of electron concentration. The squares correspond to the high-frequency mode in the 5 nm wide QW, and the circles correspond to the high-frequency mode in the 6.2 nm wide QW. The triangles correspond to the low-frequency mode in the 6.2 nm wide QW. Red symbols correspond to $\hbar v_{s^*k+q;s,k} = 1$ meV, black ones – to $\hbar v_{s^*k+q;s,k} = 0.1$ meV. Filled symbols correspond to $T_h = 4.2$ K, empty ones – to $T_h = 77$ K. Connecting lines are drawn for the convenience of perception.

It can be seen from Fig. 9 that with an increase in the electron concentration in the 6.2 nm wide QW, the threshold hole concentrations increase. Indeed the absorbed power of the plasmon wave is proportional to the sum of the real parts of the intraband and interband conductivities. At the threshold hole concentration, the negative contribution of the real part of the interband conductivity becomes equal to the positive contribution of the intraband one (Drude conductivity) at some frequency. The intraband conductivity is proportional to the concentration of electrons and therefore it grows with an increase in the concentration of electrons. To compensate for the growth of the real part of the intraband conductivity, an increase in the absolute value of the real part of the interband conductivity is required. This can be achieved by increasing the concentration of nonequilibrium holes. For the low-frequency mode, the figure shows data only for $\hbar v_{s^*k+q;s,k} = 0.1$ meV. Due to the limitation of the frequency of this mode and, accordingly, the density of states of electrons and holes in the corresponding

energy range, its amplification is possible at $\hbar v_{s^*k+q,s,k}$ less than a certain value. So at $\hbar v_{s^*k+q,s,k} = 1$ meV amplification is impossible.

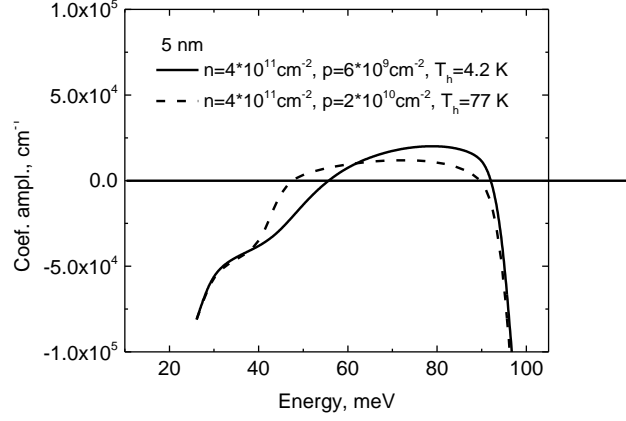


Fig. 10. Gain spectra of the high-frequency plasmon-LO mode in a 5 nm wide QW; $n = 4 \cdot 10^{11} \text{ cm}^{-2}$. Solid line: $p = 6 \cdot 10^9 \text{ cm}^{-2}$, $T_h = 4.2 \text{ K}$; dashed line: $p = 2 \cdot 10^{10} \text{ cm}^{-2}$, $T_h = 77 \text{ K}$; $\hbar v_{s^*k+q,s,k} = 1 \text{ meV}$.

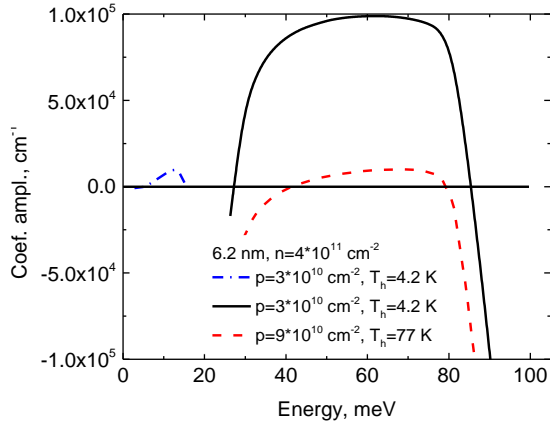


Fig. 11. Gain spectra of the plasmon-LO modes in a 6.2 nm wide QW; $n = 4 \cdot 10^{11} \text{ cm}^{-2}$. Solid and dash-dotted lines: $p = 3 \cdot 10^9 \text{ cm}^{-2}$, $T_h = 4.2 \text{ K}$, dashed line $p = 9 \cdot 10^{10} \text{ cm}^{-2}$, $T_h = 77 \text{ K}$. $\hbar v_{s^*k+q,s,k} = 1 \text{ meV}$ for the solid and dashed lines and $\hbar v_{s^*k+q,s,k} = 0.1 \text{ meV}$ for the dash-dotted line.

For the high-frequency mode, there is one more factor that leads to an increase in the threshold hole concentration with an increase in the electron concentration. One can see in Fig. 8 that at small wave vectors of holes, transitions from the conduction band to the valence band do not occur due to the impossibility of fulfilling the energy-momentum conservation laws for such transitions. In addition, the size of the vicinity of the point $k = 0$, where such transitions are forbidden, increases with increasing electron concentration. Thus, with an increase in the

electron concentration in the 6.2 nm QW, the number of holes that cannot take part in the amplification of plasmons increases.

In a 5 nm wide QW, only the high-frequency plasmon-LO phonon mode could be amplified, because the band gap in this structure exceeds the maximum quantum energy of the low-frequency mode. Fig. 9 clearly shows that, in contrast to the 6.2 nm wide QW in the 5 nm wide QW, an increase in the concentration of equilibrium electrons leads to a decrease in the threshold concentration of nonequilibrium holes. This is explained by a decrease the region of the k -space of holes near $k = 0$ where the electron-hole recombination with the plasmon emission is impossible with an increase in the electron concentration (see Fig. 6). And at electron concentration of $8 \cdot 10^{11} \text{ cm}^{-2}$, such a region is completely absent. Therefore, with an increase in the electron concentration in the 5 nm wide QW, in contrast to the 6.2 nm wide QW, the fraction of holes that can take part in the amplification of plasma oscillations increases.

Note that for an undoped 5 nm wide QW, the threshold concentration under the considered conditions is 10^{11} cm^{-2} at $\hbar v_{s',\mathbf{k}+\mathbf{q},s,\mathbf{k}} = 1 \text{ meV}$ for the conduction band and $\hbar v_{s',\mathbf{k}+\mathbf{q},s,\mathbf{k}} = 2 \text{ meV}$ for the valence band. Since there are much fewer holes than electrons, their relaxation times (as well as polarizability) practically do not affect the properties of the plasmons under consideration. Therefore, in a 5 nm QW, doping makes it possible to reduce the threshold concentration of nonequilibrium carriers by about 4 to 30 times as compared to an undoped QW.

Calculated gain spectra for 5 and 6.2 nm wide QWs at various concentrations of nonequilibrium holes are given in Fig. 10, 11. It can be seen that the gain reach values $10^4 - 10^5 \text{ cm}^{-1}$. Fig. 11 also demonstrates that the gain of the low-frequency mode is significantly lower than that of the high-frequency one.

Probably, the generation of plasmons can be observed, for example, using the plasmon resonator described in [26].

5. Conclusions

We found the spectra of the plasmon-LO phonon modes in a 6.2 nm wide HgTe gapless QW, a 5 nm wide QW with a normal band structure, and an 8 nm wide QW with an inverted band structure at three concentrations of equilibrium electrons. It is shown that, in the three considered QWs, the spectra of the plasmon-LO phonon modes differ slightly, provided that the electron concentrations in the QWs are equal. The spectra of the absorption coefficients of two-dimensional plasmons are found. It is shown that an increase in the concentration of electrons in a quantum well leads to a decrease in the absorption coefficients. The rates of recombination of nonequilibrium holes, caused by the emission of plasmon-LO phonon modes, are found. The threshold concentrations of holes, above which the plasmon amplification is possible, are calculated for various electron concentrations. It is shown that in a 5 nm wide QW, the presence of equilibrium electrons significantly reduces the threshold hole concentration required for amplification of the plasmon-LO phonon modes. It is shown that with an increase in the concentration of equilibrium electrons in the range from $2 \cdot 10^{11}$ to $8 \cdot 10^{11} \text{ cm}^{-2}$ in a structure with a gapless quantum well, the threshold concentration of holes necessary for plasmon gain increases.

Funding. The Russian Science Foundation (Grant No. 20-42-09039); the French Agence Nationale pour la Recherche (COLECTOR project).

Disclosures. The authors declare no conflicts of interest.

Data availability. Data underlying the results presented in this paper are not publicly available at this time but may be obtained from the authors upon reasonable request.

References

1. F. Rana, "Graphene Terahertz Plasmon Oscillators," *IEEE Transactions on Nanotechnology*, **7**, 91-99 (2008).
2. A. A. Dubinov, V. Ya. Aleshkin, V. Mitin, T. Otsuji, and V. Ryzhii, "Terahertz surface plasmons in optically pumped graphene structures," *J. Phys.: Condensed Matter* **23**, 145302 (2011).
3. V. V. Popov, O. V. Polischuk, A. R. Davoyan, V. Ryzhii, T. Otsuji, and M. S. Shur, "Plasmonic terahertz lasing in an array of graphene nanocavities," *Phys. Rev. B* **86**, 195437 (2012).
4. T. Watanabe, T. Fukushima, Yu. Yabe, S. A. Boubanga Tombet, A. Satou, A. A. Dubinov, V. Ya. Aleshkin, V. Mitin, V. Ryzhii, and T. Otsuji, "The gain enhancement effect of surface plasmon polaritons on terahertz stimulated emission in optically pumped monolayer graphene," *New Journal of Physics*, **15**, 075003 (2013).
5. A. A. Dubinov, V. Ya. Aleshkin, V. Ryzhii, M. S. Shur, and T. Otsuji, "Surface-plasmons lasing in double-graphene-layer structures", *J. Appl. Phys.* **115**, 044511 (2014).
6. V. Ryzhii, T. Otsuji, M. Ryzhii, A. A. Dubinov, V. Ya. Aleshkin, V. E. Karasik, and M. S. Shur, "Negative terahertz conductivity and amplification of surface plasmons in graphene-black phosphorus injection laser heterostructures," *Phys. Rev. B*, **100**, 115436 (2019).
7. T. Winzer, R. Jago, and E. Malic, "Experimentally accessible signatures of Auger scattering in graphene," *Phys. Rev. B*, **94**, 235430 (2016).
8. S. Dvoretzky, N. Mikhailov, Yu. Sidorov, V. Shvets, S. Danilov, B. Wittman, and S. Ganichev, "Growth of HgTe Quantum Wells for IR to THz Detectors," *J. Electron. Matter*, **39**, 918-923 (2010).
9. V. Ya. Aleshkin, A. A. Dubinov, V. V. Romyantsev, M. A. Fadeev, O. L. Domnina, N. N. Mikhailov, S. A. Dvoretzky, and S.V.Morozov, "Radiative recombination in narrow gap HgTe/CdHgTe quantum well heterostructures for laser applications," *J. Phys.: Condens. Matter*, **30**, 495301 (2018).
10. V. Ya. Aleshkin, V. V. Romyantsev, K. E. Kudryavtsev, A. A. Dubinov, V. V. Utochkin, M. A. Fadeev, G. Alymov, N. N. Mikhailov, S. A. Dvoretzky, F. Teppe, V. I. Gavrilenko, and S.V. Morozov, "Auger recombination in narrow gap HgCdTe/CdHgTe quantum well heterostructures," *J. Appl. Phys.* **129**, 133106 (2021).
11. K. Kapralov, G. Alymov, D. Svintsov, A. Dubinov, "Feasibility of surface plasmon lasing in HgTe quantum wells with population inversion" *J. Phys.: Condens. Matter* **32**, 065301 (2020).
12. V. Ya. Aleshkin, G. Alymov, A. A. Dubinov, V. I. Gavrilenko, and F. Teppe, "Plasmon recombination in narrowgap HgTe quantum wells," *J. Phys.: Commun.* **4**, 115012 (2020).
13. F. Stern, "Polarizability of a two-dimensional electron gas," *Phys. Rev. Lett.* **18**, 546-547 (1967).
14. J. M. Ziman, "Principles of the Theory of Solids", 2nd ed., Cambridge, UK, Cambridge University Press, 1972, ch. 5, pp. 146-149.
15. V. Ya. Aleshkin, A. A. Dubinov, V. I. Gavrilenko, and F. Teppe, "Stimulated emission of plasmon-LO mode in narrow gap HgTe/CdHgTe quantum wells," arXiv: 2106.04848 [cond-mat.mes-hall].
16. J. Polit, "Model of the two well potential for Hg-atoms in the Hg_{1-x}Cd_xTe alloy lattice," *Bull. Polish Acad. Sciences. Tech. Sciences.* **59**, 331-341 (2011).
17. G. M. Minkov, A. V. Germanenko, O. E. Rut, A. A. Sherstobitov, M. O. Nestoklon, S. A. Dvoretzki, and N. N. Mikhailov, "Spin-orbit splitting of valence and conduction bands in HgTe quantum wells near the Dirac point," *Phys. Rev. B*, **93**, 155304 (2016).
18. S. A. Tarasenko, M. V. Durnev, M. O. Nestoklon, E. L. Ivchenko, J.-W. Luo, and A. Zunger, "Split Dirac cones in HgTe/CdTe quantum wells due to symmetry-enforced level anticrossing at interfaces," *Phys. Rev. B*, **91**, 081302(R) (2015).
19. M. Zholudev, F. Teppe, M. Orlita, C. Consejo, J. Torres, N. Dyakonova, M. Czapkiewicz, J. Wrobel, G. Grabecki, N. Mikhailov, S. Dvoretzki, A. Ikonnikov, K. Spirin, V. Aleshkin, V. Gavrilenko, and W. Knap, "Magnetospectroscopy of two-dimensional HgTe-based topological insulators around the critical thickness," *Phys. Rev. B*, **86**, 205420 (2012).
20. K. E. Kudryavtsev, V. V. Romyantsev, V. Ya. Aleshkin, A. A. Dubinov, V. V. Utochkin, M. A. Fadeev, N. N. Mikhailov, G. Alymov, D. Svintsov, V.I. Gavrilenko, and S. V. Morozov, "Temperature limitations for stimulated emission in 3–4 μm range due to threshold and non-threshold Auger recombination in HgTe/CdHgTe quantum wells," *Appl. Phys. Lett.*, **117**, 083103 (2020).
21. S. V. Morozov, V. V. Romyantsev, M. A. Fadeev, M. S. Zholudev, K. E. Kudryavtsev, A. V. Antonov, A. M. Kadykov, A. A. Dubinov, N. N. Mikhailov, S. A. Dvoretzki, and V. I. Gavrilenko, "Stimulated emission from HgCdTe quantum well heterostructures at wavelengths up to 19.5 μm," *Appl. Phys. Lett.*, **111**, 192101 (2017).
22. S. V. Morozov, V. V. Romyantsev, A. M. Kadykov, A. A. Dubinov, K. E. Kudryavtsev, A. V. Antonov, N. N. Mikhailov, S. A. Dvoretzki, and V. I. Gavrilenko, "Long wavelength stimulated emission up to 9.5 μm from HgCdTe quantum well heterostructures," *Appl. Phys. Lett.*, **108**, 092104 (2016).
23. P. Yu, and M. Cardona, "Fundamentals of Semiconductors," 4th ed., Heidelberg, Springer 2010, ch 6, pp. 337-338.
24. G. M. Minkov, V. Ya. Aleshkin, O. E. Rut, A. A. Sherstobitov, A. V. Germanenko, S. A. Dvoretzki, and N. N. Mikhailov, "Electron mass in a HgTe quantum well: Experiment versus theory," *Physica E* **116**, 113742 (2020).
25. S. Kohen, B. S. Williams, Q. Hu, "Electromagnetic modeling of terahertz quantum cascade laser waveguides and resonators," *J. Appl. Phys.* **97**, 053106 (2005).
26. V. Gilberti, A. Di Gaspare, E. Giovine, M. Ortolani, L. Sorba, G. Biasiol, V.V.Popov, D.V.Fateev, F. Evangelisti, "Downconversion of terahertz radiation due to intrinsic hydrodynamic nonlinearity of a two-dimensional electron plasma", *Phys. Rev. B* **91**, 165313 (2015).